J. Appl. Math. & Informatics Vol. **39***(2021), No. 1 - 2, pp. 31 - 43*
https://doi.org/10.14317/jami.2021.031

EFFECTS OF ANGULAR VELOCITY AND BOUNDARY TEMPERATURE TO THERMO-ELASTIC CHARACTERISTICS ON HOMOGENEOUS CIRCULAR DISKS SUBJECTING TO CONTACT FORCES[†]

JAEGWI GO

Abstract. A homogeneous circular disk undergoing a contact force is considered to investigate the thermo-elastic characteristics, and the inquiry is based on the variations of outer surface temperature and angular velocity. The intensity of stresses grows with the increase of outer surface temperature, and the circumferential strain reacts more sensitively to the change of outer surface temperature than the radial strain. In general, higher angular velocity produces; (i) larger expansion in the radial direction, (ii) smaller displacement in the circumferential, (iii) diminished intensity in the stresses. It is demonstrated that outer surface temperature and angular velocity are critical factors in the determination of thermo-elastic characteristics of homogeneous circular disks subjecting to a contact force. The results obtained can be applied on the design of a homogeneous circular cutter to promote proper and reliable thermos-elastic characteristics in service by the proper operation of these parameters.

AMS Mathematics Subject Classification : 74E05, 74F05.
Key words and phrases : Angular velocity, Circular disk, Contact force, Thermo-elastic characteristic, Finite volume method.

1. Introduction

Rotating circular disks subjecting to contact forces are always exposed to the risk of friction, wear, heat generation, and temperature deformation, which cause complex mutual interactions. The complicated interactions developed by the variation of each parameter are crucial factors to be considered in the study of the thermo-elastic movements. The investigation to the influences of angular

Received September 14, 2020. Revised November 2, 2020. Accepted November 3, 2020.
[†]This research was supported by Basic Science Research Program through the National Research Foundation of Korea (NRF) funded by the Ministry of Education (NRF-2018R1D1A1B07043714).

velocity and outer boundary temperature in rotating circular disk under the loading of contact forces still remains as a challenging work.

Since circular disk is a practically useful shape in various industrial applications, circular shaped model is a popular target model and the physical movements have been investigated by many researchers. Obata and Noda [1] studied the steady thermal stress in a hollow circular cylinder and sphere, and Liew et al. [2] analyzed thermal stress behavior of functionally graded hollow circular cylinders. By Kovalyshen [3], a circular disk cutter is characterized the movements of an oscillatory in operating process reduces cutting forces, and the radial component effects of the reaction force on the bending of thin circular plates are described by Huang and Li [4] applying Kirchhoff plate theory. One of major reason to the cutting ring breakage is the unbalance forces between two sides of cutter ring during cutting process, which is proved by Ren et al. [5]. With a forced condition of complicated stress fields for an edge-cracked circular disk Wu and Tong determined stress intensity factors crack opening displacements using Weight function method [6].

However, even though contact force is a crucial parameter in determination of the thermo-elastic characteristics, most of researches for the circular disks have been carried out without considering contact force during the cutting process. Rad [7] investigated, based on poroelasticity theory, static behavior of the auxetic-porous structures composed of multi directional heterogeneous materials with considering friction force. Applying the yaw angle misalignment theory to rotary contact systems for circular sliding contact Tadokoro et al. [8] testified the followings: parallel misalignment between drive and driven shafts stabilize the systems by dint of change in the direction of local frictional force.

In the present research, focused factors are the angular velocity and outer temperature and the influences to thermo-elastic characteristics, according to the variation of them, are analyzed on a rotating Al homogeneous circular disk undergoing of a contact force. Hooke's law is used to drive a pair of partial differential equations under the consideration of contact forces. Due to the complicated governing equations a finite volume method is applied to obtain the solution of displacement, stress, and stain components as a function of angular velocity and outer boundary temperature.

2. Mathematical Modelling

A rotating homogeneous circular disk is considered. The disk is of a concentric circular hole and undergoes contact forces. The origin of the polar coordinate system $r-\theta$ is assumed to be located at the center of the disk and hole, and the radii of the hole and outer surface of the disk are designated by a and b (see Fig. 1). The following nomenclatures are used in the derivation of governing equations.

u: radial displacement component
v: circumferential displacement component
ε_r: radial strain
ε_θ: circumferential strain

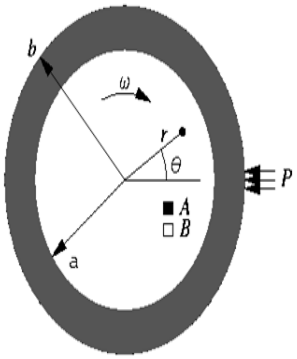

FIGURE 1. Schematic diagram of homogeneous circular disk models.

γ: shearing strain
σ_θ: circumferential stress
ν: Poisson's ratio
N: revolutions per minute (rpm)
α: coefficient of thermal expansion
σ_r: radial stress
τ: shearing stress
ω: angular velocity
E: Young's modulus
ρ: density of the disk

2.1. Temperature distribution profiles

Due to the assumption that the circular disk undergoes the loading of symmetric temperature to the radial direction only, the differential equation for the temperature distribution in the polar coordinate can be expressed with

$$\frac{1}{r}\frac{\partial}{\partial r}(r\frac{\partial T}{\partial r}) = 0. \tag{1}$$

The general solution of Eq.(1) is of the form

$$T(r) = c_1 \ln r + c_2, \tag{2}$$

where c_1 and c_2 are integral constants and will be obtained based on the boundary conditions.

2.2. Mathematical formulation

Hooke's law in plane stress problems yields the following strain-stress relations for the circular disk undergoing thermal expansion, in polar coordinates,

$$\epsilon_r = \frac{1}{E}[\sigma_r - \nu\sigma_\theta] + \alpha T \qquad \epsilon_\theta = \frac{1}{E}[\sigma_\theta - \nu\sigma_r] + \alpha T$$
$$\tau_{r\theta} = \frac{E}{2(1+\nu)}\gamma_{r\theta} \qquad \tau_{z\theta} = 0 \qquad \tau_{rz} = 0. \tag{3}$$

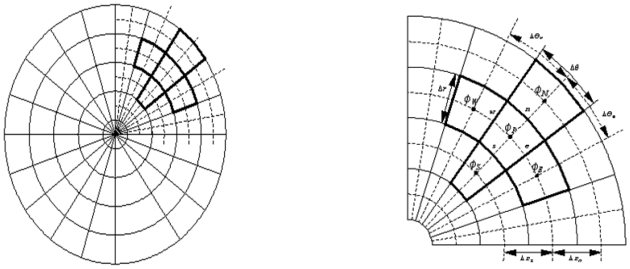

(a) (b)

FIGURE 2. (a) Discretization of circular disk domain, (b) Notations of finite control volumes.

The $T(r)$ denotes the change in temperature at any distance . The strain components are expressed with the deformation components as follows:

$$\epsilon_r = \frac{\partial u}{\partial r} \qquad \epsilon_\theta = \frac{1}{r}\frac{\partial v}{\partial \theta} + \frac{u}{r} \qquad \epsilon_z = 0$$
$$\gamma_{r\theta} = \frac{1}{r}\frac{\partial u}{\partial \theta} + \frac{\partial v}{\partial r} - \frac{v}{r} \qquad \gamma_{z\theta} = 0 \qquad \gamma_{rz} = 0. \tag{4}$$

Since equilibrium equations in polar coordinates are

$$\frac{\partial \sigma_r}{\partial r} + \frac{1}{r}\frac{\partial \tau_{r\theta}}{\partial \theta} + \frac{\sigma_r - \sigma_\theta}{r} + \rho\omega^2 r = 0$$
$$\frac{\partial \sigma_\theta}{\partial \theta} + r\frac{\partial \tau_{r\theta}}{\partial r} + 2\tau_{r\theta} = 0, \tag{5}$$

the combination of equations Eq.(3) - Eq.(5) provides the governing partial differential equations system

$$\frac{\partial}{\partial r}(r\frac{\partial u}{\partial r}) + \frac{1-\nu}{2r}\frac{\partial^2 u}{\partial \theta^2} - \frac{3-\nu}{2r}\frac{\partial v}{\partial \theta} + \frac{1+\nu}{2}\frac{\partial^2 v}{\partial r \partial \theta} - \frac{u}{r} + \frac{1-\nu^2}{E}\rho\omega^2 r^2$$
$$= (1+\nu)\alpha r\frac{dT}{dr}$$
$$\frac{1-\nu}{2}\frac{\partial}{\partial r}(r\frac{\partial v}{\partial r}) + \frac{1}{r}\frac{\partial^2 v}{\partial \theta^2} + \frac{3-\nu}{2r}\frac{\partial u}{\partial \theta} + \frac{1+\nu}{2}\frac{\partial^2 u}{\partial r \partial \theta} - \frac{1-\nu}{2}\frac{v}{r} = 0. \tag{6}$$

The thermo-elastic characteristics of a present circular disk subjecting to contact forces are investigated based on the following boundary conditions

$$\sigma_r(a,\theta) = 0 \qquad \sigma_r(b, \theta - \{0\}) = 0 \qquad \sigma_r(b,0) = P \quad \textit{at contact point.}$$

2.3. Finite volume formulation

The governing partial differential equations system is too involved to obtain analytic solution, and a finite volume method thus is adopted for the approximation. The domain is divided up into control volume and integrates the field equations over each control volume to be applied for approximated solutions (see Fig. 2). The (i, j) represents the finite surface mesh and the discretizations for the governing equations are appeared on the basis of the following relations at the adjacent locations;

$$
\begin{aligned}
&(\frac{\partial u}{\partial r})_{i,j+\frac{1}{2}} = \frac{u_{i,j+1} - u_{i,j}}{\Delta r} \qquad (\frac{\partial u}{\partial r})_{i,j-\frac{1}{2}} = \frac{u_{i,j} - u_{i,j-1}}{\Delta r} \\
&\qquad (\frac{\partial u}{\partial r})_{i,j-1} = \frac{u_{i,j+1} - u_{i,j-1}}{2\Delta r} \\
&(\frac{\partial w}{\partial z})_{i,j} = \frac{1}{2\Delta z}(3w_{i,j} - 4w_{i-1,j} + w_{i-2,j}) \\
&w_{i+\frac{1}{2},j+1} = w_{i,j+1} + \frac{1}{4}(3w_{i,j+1} - 4w_{i-1,j+1} + w_{i-2,j+1}) \\
&w_{i-\frac{1}{2},j+1} = w_{i-1,j+1} + \frac{1}{4}(w_{i,j+1} - w_{i-2,j+1}) \\
&\phi_{i+\frac{1}{2},j+\frac{1}{2}} = \frac{1}{2}(\phi_{i+\frac{1}{2},j+1} - \phi_{i+\frac{1}{2},j}).
\end{aligned} \tag{7}
$$

The subscript 1/2 implies the value of the displacement at the boundary of the control surface (see Fig. 2(b)). Thus, the governing equations are discretized as below

$$
\begin{aligned}
&A_{11}u_{i+1,j} + A_{12}u_{i,j+1} + A_{13}u_{i,j} + A_{14}u_{i,j-1} + A_{15}u_{i-1,j} + B_{11}v_{i,j+1} \\
&+B_{12}v_{i,j} + B_{13}v_{i,j-1} + B_{14}v_{i-1,j+1} + B_{15}v_{i-1,j} + B_{16}v_{i-1,j-1} \\
&+B_{17}v_{i-2,j+1} + B_{18}v_{i-2,j} + B_{19}v_{i-2,j-1} = f_{i,j} \\
&A_{21}u_{i,j+1} + A_{22}u_{i,j} + A_{23}u_{i,j-1} + A_{24}u_{i-1,j+1} + A_{25}u_{i-1,j} + A_{26}u_{i-1,j-1} \\
&+A_{27}u_{i-2,j+1} + A_{28}u_{i-2,j} + A_{29}u_{i-2,j-1} + B_{21}v_{i+1,j} + B_{22}v_{i,j+1} \\
&+B_{23}v_{i,j} + B_{24}v_{i,j-1} + B_{25}v_{i-1,j} = 0,
\end{aligned} \tag{8}
$$

where

$$
\begin{aligned}
&A_{11} = \frac{1-\nu}{2}\frac{\Delta r}{\Delta\theta}\frac{1}{r_{i,j}},\ A_{12} = \frac{\Delta\theta}{\Delta r}r_{i,j+\frac{1}{2}},\ A_{14} = \frac{\Delta\theta}{\Delta r}r_{i,j-\frac{1}{2}},\ A_{15} = \frac{1-\nu}{2}\frac{\Delta r}{\Delta\theta}\frac{1}{r_{i,j}}, \\
&A_{13} = -\frac{\Delta\theta}{\Delta r}(r_{i,j+\frac{1}{2}} + r_{i,j-\frac{1}{2}}) - (1-\nu)\frac{\Delta r}{\Delta\theta}\frac{1}{r_{i,j}} - \Delta r\Delta\theta\frac{1}{r_{i,j}}, \\
&B_{11} = \frac{3}{8}(1+\nu),\ B_{12} = -\frac{3}{4}(3-\nu)\Delta r\frac{1}{r_{i,j}},\ B_{13} = -\frac{7}{16}(1+\nu), \\
&B_{14} = -\frac{1}{2}(1+\nu),\ B_{15} = \frac{5}{2}(3-\nu)\frac{1}{r_{i,j}},\ B_{16} = \frac{9}{16}(1+\nu),
\end{aligned}
$$

TABLE 1. Mechanical and thermal properties for thermoelastic characteristics of rotating FG circular disks.

Material / Property	Elastic module (MPa)	Thermal expansion coefficient $(10^{-6}/^oC)$	Thermal conductivity $(W/M-^oC)$	Density (g/cm^3)
Al	71	23.1	237	2.7

$$B_{17} = \frac{1}{8}(1+\nu),\ \ B_{18} = -\frac{3}{4}(3-\nu)\Delta r\frac{1}{r_{i,j}},\ \ B_{19} = -\frac{1}{8}(1+\nu),$$
$$f_{i,j} = (1+\nu)\alpha r_{i,j}\Delta\theta(T_{i,j+\frac{1}{2}} - T_{i,j-\frac{1}{2}}) - \Delta r\Delta\theta\rho\omega^2\frac{1-\nu^2}{E}r_{i,j}^2,$$

$$A_{21} = \frac{3}{8}(1+\nu),\ \ A_{22} = \frac{3}{4}(3-\nu)\Delta r\frac{1}{r_{i,j}},\ \ A_{23} = -\frac{7}{16}(1+\nu),$$
$$A_{24} = -\frac{1}{2}(1+\nu),\ \ A_{25} = -(3-\nu)\Delta r\frac{1}{r_{i,j}},\ \ A_{26} = \frac{9}{16}(1+\nu),$$
$$A_{27} = \frac{1}{8}(1+\nu),\ \ A_{28} = (3-\nu)\Delta r\frac{1}{r_{i,j}},\ \ A_{29} = -\frac{1}{8}(1+\nu),$$
$$B_{21} = \frac{\Delta r}{\Delta\theta}\frac{1}{r_{i,j}},\ \ B_{22} = \frac{\Delta\theta}{\Delta r}r_{i,j+\frac{1}{2}},\ \ B_{24} = \frac{\Delta\theta}{\Delta r}r_{i,j+\frac{1}{2}},\ \ B_{25} = \frac{\Delta r}{\Delta\theta}\frac{1}{r_{i,j}},$$
$$B_{23} = -\frac{\Delta\theta}{\Delta r}(r_{i,j+\frac{1}{2}} + r_{i,j-\frac{1}{2}}) - \frac{1-\nu}{2}\Delta r\Delta\theta - 2\frac{\Delta r}{\Delta\theta}\frac{1}{r_{i,j}}.$$

3. Numerical results and discussions

The temperature distribution profiles are displayed using the differential equation induced in section 2.1 according to the inner and outer boundary conditions. The T_a and T_b represent the temperature degree of inner and outer boundaries, respectively. The finite volume formula developed in section 2.3 are employed to obtain numerical approximations for the displacement, stress, and strain components of an Al homogeneous circular disk. The mechanical and thermal properties of the ingredient material are shown in Table 1. For the study of the influences of outer boundary variation the representative outer surface temperature values T_b=150, T_b=300, T_b=450, T_b=600 are chosen. The temperature distribution profiles are displayed in Fig. 3 for various outer boundary temperature values when the inner surface temperature T_a=20 . Higher temperature distribution appears with the increase of outer surface temperature, and logarithmic growths exhibit along the normalized radius $r-a/b-a$ in the temperature distribution profiles, as shown in equation (2).

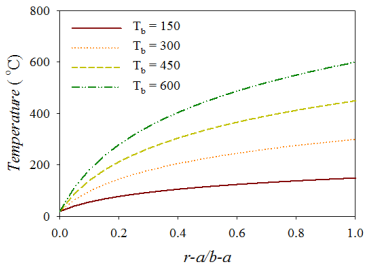

FIGURE 3. Temperature distribution along the radial direction.

The effects of outer surface temperature to thermo-elastic characteristics are expressed through Fig. 4 to 6. The influences to the displacement distributions are explained in Fig. 4. As shown in Fig. 4(a), the radial displacement of the circular disk at the contact point θ=0 extends the concentric hole direction until around $r-a/b-a$=0.9 and sudden shift to the outer boundary direction engenders after $r-a/b-a$=0.9. As the growth of outer surface temperature larger expansion appears in the radial displacement magnitude and the largest displacement occurs at the contact point of T_b=600. At θ=180, larger expansion is produced to the concentric hole direction and the largest radial displacement is detected around $r-a/b-a$=0.3 of T_b=600 in magnitude (see Fig. 4(b)). The circumferential displacement are presented at the normalized radius values $r-a/b-a=0.1$ and 0.9. Near domain of the disk inner surface is susceptible to the change of outer boundary temperature and negative circumferential displacement exhibits (see Fig. 4(c)). The circumferential displacement increases along the growth of outer surface temperature the largest expansion occurs around θ=0.5 radian of T_b=600. Near outer boundary of the circular disk the circumferential displacement fluctuates to both positive and negative directions (see Fig. 4(d)). But, the outer surface temperature variation effects to circumferential displacement is not serious and the influences of temperature variation appears after θ=1 radian.

The influences of outer surface temperature variation to stress distributions are displayed in Fig. 5. At θ=0, the radial stress is not susceptible to the change of outer surface temperature over entire domain except both disk boundaries (see Fig. 5(a)). The magnitude of the radial stress increases with the growth of outer surface temperature. But, at θ=180, the effect of outer surface temperature variation is notable. With the increase of outer surface temperature, inner boundary undergoes higher compressive radial stress and larger tensile radial stress develops at outer boundary (see Fig. 5(b)). As shown in Fig. 5(c), the disk experiences the compressive circumferential stress at the normalized radius $r-a/b-a=0.1$ over all area. The intensity of the compressive circumferential

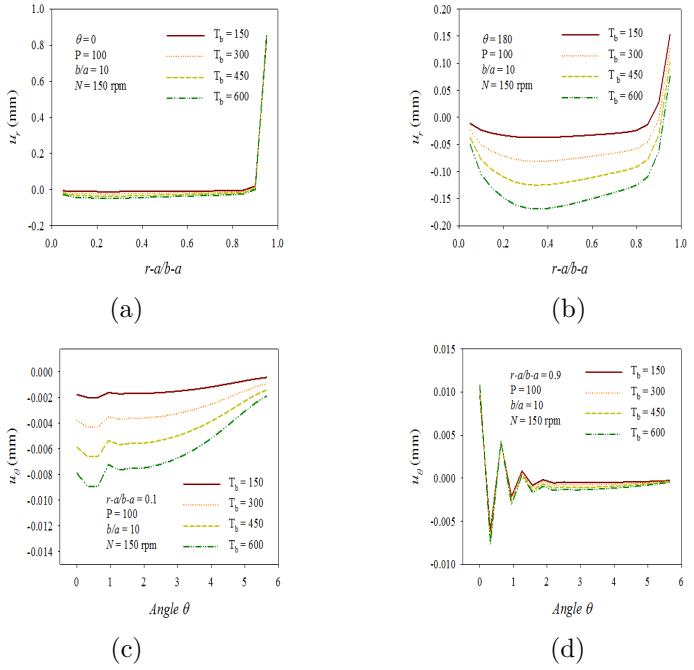

FIGURE 4. Effects of outer boundary temperature on the displacement component: (a) radial at θ=0, (b) radial at θ=180, (c) circumferential at $r-a/b-a=0.1$, (d) circumferential at $r-a/b-a=0.9$.

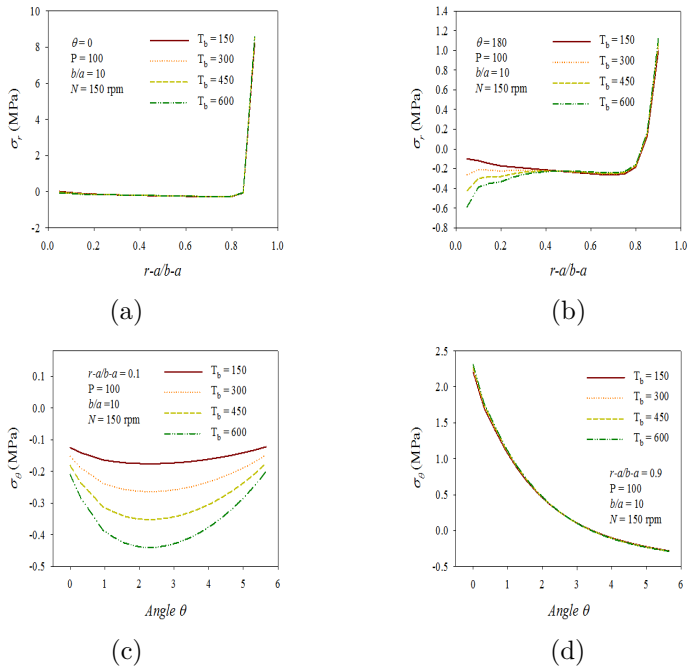

FIGURE 5. Effects of outer boundary temperature on the stress component: (a) radial at θ=0, (b) radial at θ=180, (c) circumferential at $r-a/b-a=0.1$, (d) circumferential at $r-a/b-a=0.9$.

stress grows as outer surface temperature increases and the largest circumferential stress occurs around θ=2 radian of T_b=600. At $r - a/b - a = 0.9$, the effect of outer surface temperature change is minor and only near area of the contact point shows little impact (see Fig. 5(d)). Fig. 6 presents the influences of outer surface temperature variation to the strain distributions. As shown in Fig. 6(a), outer surface temperature variation is not a critical factor at the contact point and trivial impact appears on the radial strain distributions. But, at θ=180, the circumferential strain distribution over near area of the inner boundary is sensitive to the change of outer boundary temperature. The magnitude of the radial strain is getting larger with the growth of outer surface temperature (see Fig. 6(b)). The circumferential strain reacts sensitively to the change of outer boundary temperature at $r - a/b - a = 0.1$. The circumferential strain increases as outer boundary temperature increases, and the largest circumferential strain occurs around θ=2 radian of T_b=600 (see Fig. 6(c)). Near area of the outer boundary exhibits a different behavior in the circumferential strain distributions. Positive values are converted into negative in the circumferential strain as the outer surface temperature increases, and the circumferential strain fluctuates over near area around θ=0.

The effects of angular velocity to thermo-elastic characteristics are presented through Fig. 7 to 9. The representative values of revolutions per minute N=150, N=300, N=600, and N=1000 are chosen for the influences of angular velocity. The displacement distributions in response to the change of angular velocity are presented in Fig. 7. At θ=0, the effect of angular velocity to the radial displacement is minor and a little larger difference is produced over area of $0.2 < r - a/b - a < 0.9$ in the radial displacement with the growth of angular velocity (see Fig. 7(a)). But, the variation of angular velocity produces notable influences at θ=180 (see Fig. 7(b)). With the increase of angular velocity larger radial displacement develops to outer boundary direction, and the area around $r - a/b - a = 0.8$ is the most sensitive part to the change of angular velocity. As shown in Fig. 7(c), the circumferential displacement is susceptible to angular velocity variation over near area of inner surface. The intensity of the circumferential displacement decreases as angular velocity increases and the largest magnitude occurs of N=150. Similar behavior appears in the intensity of the circumferential displacement over near area of outer surface (see Fig. 7(d)). But, the variation of angular velocity causes minor effects in the circumferential displacement.

Fig. 8 displays the effects of angular velocity to the stresses. The variation of angular velocity produces trivial influence to the radial stress at the contact point (see Fig. 8(a)). But, at θ=180, the intensity of angular velocity is indispensable and the increase of angular velocity generates smaller compressive radial stresses until around $r - a/b - a = 0.8$ (see Fig. 8(b)). At $r - a/b - a = 0.1$, the change of angular velocity yields considerable impact to the circumferential stress (see Fig. 8(c)). The magnitude of the compressive circumferential stress decreases with the growth of angular velocity. But, as shown in Fig. 8(d),

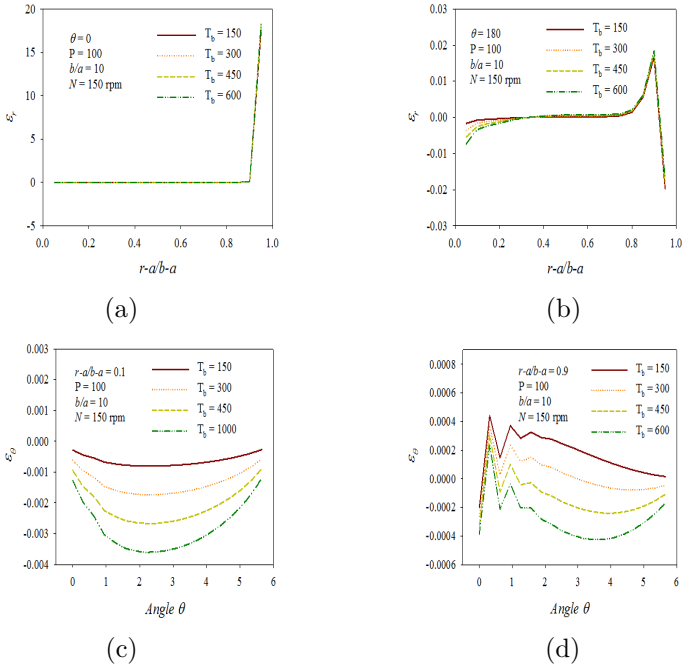

FIGURE 6. Effects of outer boundary temperature on the strain component: (a) radial at θ=0, (b) radial at θ=180, (c) circumferential at $r - a/b - a = 0.1$, (d) circumferential at $r - a/b - a = 0.9$.

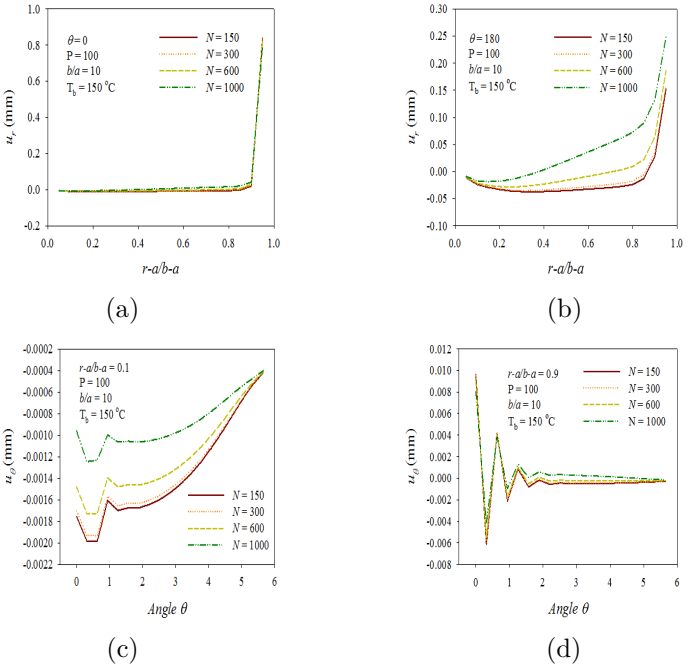

FIGURE 7. Effects of angular velocity on the displacement component: (a) radial at θ=0, (b) radial at θ=180, (c) circumferential at $r - a/b - a = 0.1$, (d) circumferential at $r - a/b - a = 0.9$.

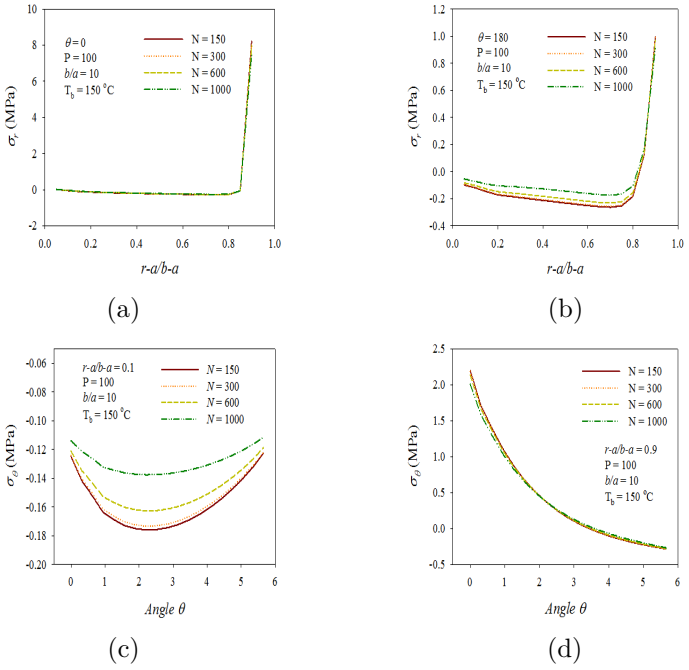

FIGURE 8. Effects of angular velocity on the stress component: (a) radial at θ=0, (b) radial at θ=180, (c) circumferential at $r - a/b - a = 0.1$, (d) circumferential at $r - a/b - a = 0.9$.

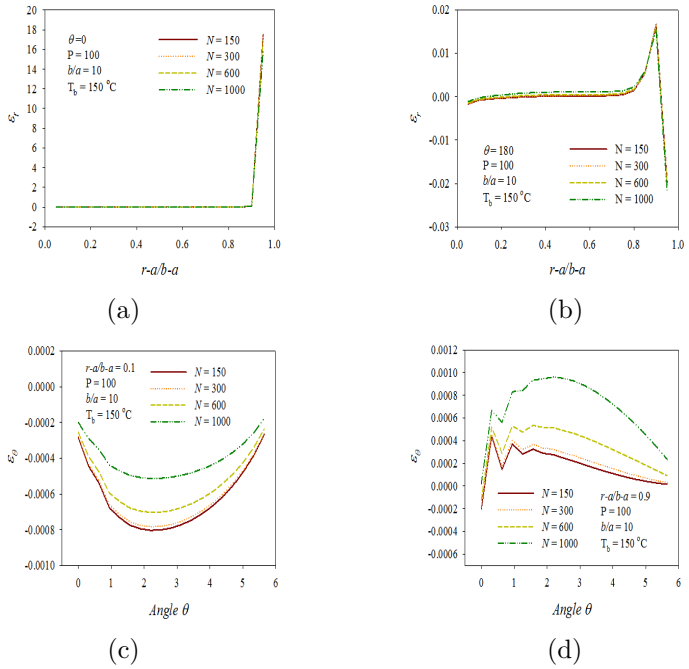

FIGURE 9. Effects of angular velocity on the strain component: (a) radial at θ=0, (b) radial at θ=180, (c) circumferential at $r - a/b - a = 0.1$, (d) circumferential at $r - a/b - a = 0.9$.

different phase develops at $r-a/b-a=0.9$. The intensity of tensile circumferential stress decreases until θ=2 radian, whereas opposite phenomenon appears after θ=2 radian, with the growth of angular velocity. Fig. 9 exhibits the influences of angular velocity to the strains. The variation of angular velocity is not critical parameter in the radial strain distributions and the effects are trivial (see Figs. 9(a) and 9(b)). But, angular velocity is indispensable parameter to the circumferential strain. As shown in Figs. 9(c) and 9(d), the intensity of the circumferential strain reduces over near area of inner boundary, while the magnitude of the circumferential strain grows, as the value of angular velocity grows.

4. Conclusions

The thermo-elastic characteristics on homogeneous circular disk subjecting to a contact force have been investigated due to the variation of outer surface temperature and angular velocity. The impacts of compressive and tensile stresses grow in the radial and circumferential stresses as outer surface temperature increases. The circumferential strain is more susceptible to the change of outer surface temperature than the radial strain, and the strain distribution develops to the negative direction with the growth of outer surface temperature. Higher angular velocity produces larger expansion in the radial direction, whereas the circumferential displacement decreases with the increase of angular velocity. In general, the magnitudes of both the radial and circumferential stresses diminish when higher angular velocity is provided on the circular disk. The influence of angular velocity to the radial strain is minor, while sensitive reactions occur in the circumferential strain according to the change of angular velocity. It is demonstrated that outer surface temperature and angular velocity are important factors in the determination of thermo-elastic characteristics of homogeneous circular disks subjecting to a contact force, and the thermo-elastic behavior can be controlled by the proper operation of these parameters. Therefore, the results obtained in this study can be applied on the design of a homogeneous circular cutter or grinding disk undergoing a loading pressure to promote proper and reliable thermos-elastic characteristics in service.

References

1. Y. Obata and N. Noda, *Steady thermal stress in a hollow circular cylinder and a hollow sphere of a functionally gradient materials*, J. Therm. Stress **17** (1994), 471-487.
2. K.M. Liew, S. Kitipornchai, X.Z. Zhang, and C.W. Lim, *Analysis of the thermal stress behavior of functionally graded hollow circular cylinders*, Int. J. Solids Struct. **40** (2003), 2355-2380.
3. Y. Kovalyshen, *Analytical model of oscillatory disc cutting*, Int. J. Rock Mechanics & Mining Sciences **77** (2015), 378-383.

4. Y. Huang and X.-F. Li, *Effect of radial reaction force on the bending of circular plates resting on a ring support*, Int. J. Mechanical Sciences **119** (2016), 197-207.
5. D.-J. Ren, J.S. Shen, J.-C. Chai, and A. Zhou, *Analysis of disc cutter failure in shield tunneling using 3D circular cutting theory*, Engineering Failure Analysis **90** (2018), 23-35.
6. X.R. Wu and D.H. Tong, *Evaluation of various analytical weight function methods base on exact K-solutions of an edge-cracked circular disc*, Engineering Fracture Mechanics **189** (2018), 64-80.
7. A.B. Rad, *Static analysis of non-uniform 2D functionally graded auxetic-porous circular plates interacting with the gradient elastic foundations involving friction force*, Aerospace Science and Technology **76** (2018), 315-339.
8. C. Tadokoro, T. Nagamine, and K. Nakano, *Stabilizing effect arising from parallel misalignment in circular sliding contact*, Tribology International **120** (2018), 16-22.

Data Availability

All data included in this study are available from the corresponding author upon request.

Jaegwi Go received Ph.D. at Michigan State University. His research interests include biomathmatics, composite and functionally graded materials, elastic maerials.

Department of Mathematics, Changwon National University, Changwon 51140, Korea.
e-mail: jggo@changwon.ac.kr